ACS APPLIED MATERIALS & INTERFACES

Research Article

www.acsami.org

Enhanced Mobility and Effective Control of Threshold Voltage in P3HT-Based Field-Effect Transistors via Inclusion of Oligothiophenes

Ping-Hsun Chu,[†] Lei Zhang,[‡] Nicholas S. Colella,[‡] Boyi Fu,[†] Jung Ok Park,[§] Mohan Srinivasarao,[§,∥] Alejandro L. Briseño,[‡] and Elsa Reichmanis*[,†,§,∥]

[†]School of Chemical and Biomolecular Engineering, Georgia Institute of Technology, 311 Ferst Drive, Atlanta, Georgia 30332-0100, United States

[‡]Department of Polymer Science and Engineering, Conte Research Center, University of Massachusetts, 120 Governors Drive, Amherst, Massachusetts 01002, United States

[§]School of Materials Science and Engineering, Georgia Institute of Technology, 771 Ferst Drive, Atlanta, Georgia 30332-0245, United States

[∥]School of Chemistry and Biochemistry, Georgia Institute of Technology, 901 Atlantic Drive, Atlanta, Georgia 30332-0400, United States

Supporting Information

ABSTRACT: Improved organic field-effect transistor (OFET) performance through a polymer-oligomer semiconductor blend approach is demonstrated. Incorporation of 2,5-bis(3-dodecylthiophen-2-yl)thieno[3,2-*b*]thiophene (BTTT) into poly(3-hexylthiophene) (P3HT) thin films leads to approximately a 5-fold increase in charge carrier mobility, a 10-fold increase in current on−off ratio, and concomitantly, a decreased threshold voltage to as low as 1.7 V in comparison to single component thin films. The blend approach required no pre- and/or post treatments, and processing was conducted under ambient conditions. The correlation of crystallinity, surface morphology and photophysical properties of the blend thin films was systematically investigated via X-ray diffraction, atomic force microscopy and optical absorption measurements respectively, as a function of blend composition. The dependence of thin-film morphology on the blend composition is illustrated for the P3HT:BTTT system. The blend approach provides an alternative avenue to combine the advantageous properties of conjugated polymers and oligomers for optimized semiconductor performance.

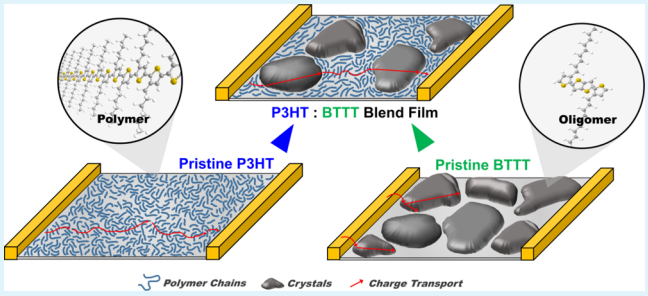

KEYWORDS: *threshold voltage, polymer-oligomer blend, poly(3-hexylthiophene), charge transport, organic field effect transistors*

INTRODUCTION

Organic field-effect transistors (OFETs) have attracted considerable attention because of their facile processability, chemical tunability, potential for low-cost, high-throughput fabrication over large-area flexible plastic substrates, and compatibility with a wide range of optoelectronic devices, such as flat-panel displays, disposable sensors, radio frequency identification tags, and so forth.[1−4] P3HT is a commercially available and widely investigated hole transport conjugated polymer, which lends itself to investigation of the correlation between thin-film microstructure and charge-transport performance. To date, many different processing methods have been proposed, such as poor solvent addition,[5] shear-induction,[6] and ultrasonication,[7] with the aim of increasing P3HT chain ordering and alignment, thus enhancing effective charge carrier transport within the polymer films.

In addition, intrinsic molecular parameters such as molecular weight (MW) and regioregularity (RR) play a crucial role in conjugated polymer supramolecular assembly and resultant charge-transport properties.[8−12] For example, Kline et al.[13] reported that the low MW samples with higher degree of crystallinity have mobilities much lower than high MW P3HT thin films with a relatively amorphous structure. The more defined grain boundaries between rodlike crystals in the low MW films were responsible for their low mobility. In contrast, the longer chains associated with high MW polymer thin films facilitated the connectivity between the ordered regions and provided a pathway for effective charge transport. The longer chains also increased opportunities for charge hopping to neighboring chains, resulting in increased mobility.

Although conjugated polymer semiconductors can have certain processing and morphological advantages over their oligomer counterparts, polymers have their own issues. For instance, chain entanglement, chain folding, and broad

Received: December 24, 2014
Accepted: March 10, 2015
Published: March 10, 2015

DOI: 10.1021/am509090j
ACS Appl. Mater. Interfaces 2015, 7, 6652−6660

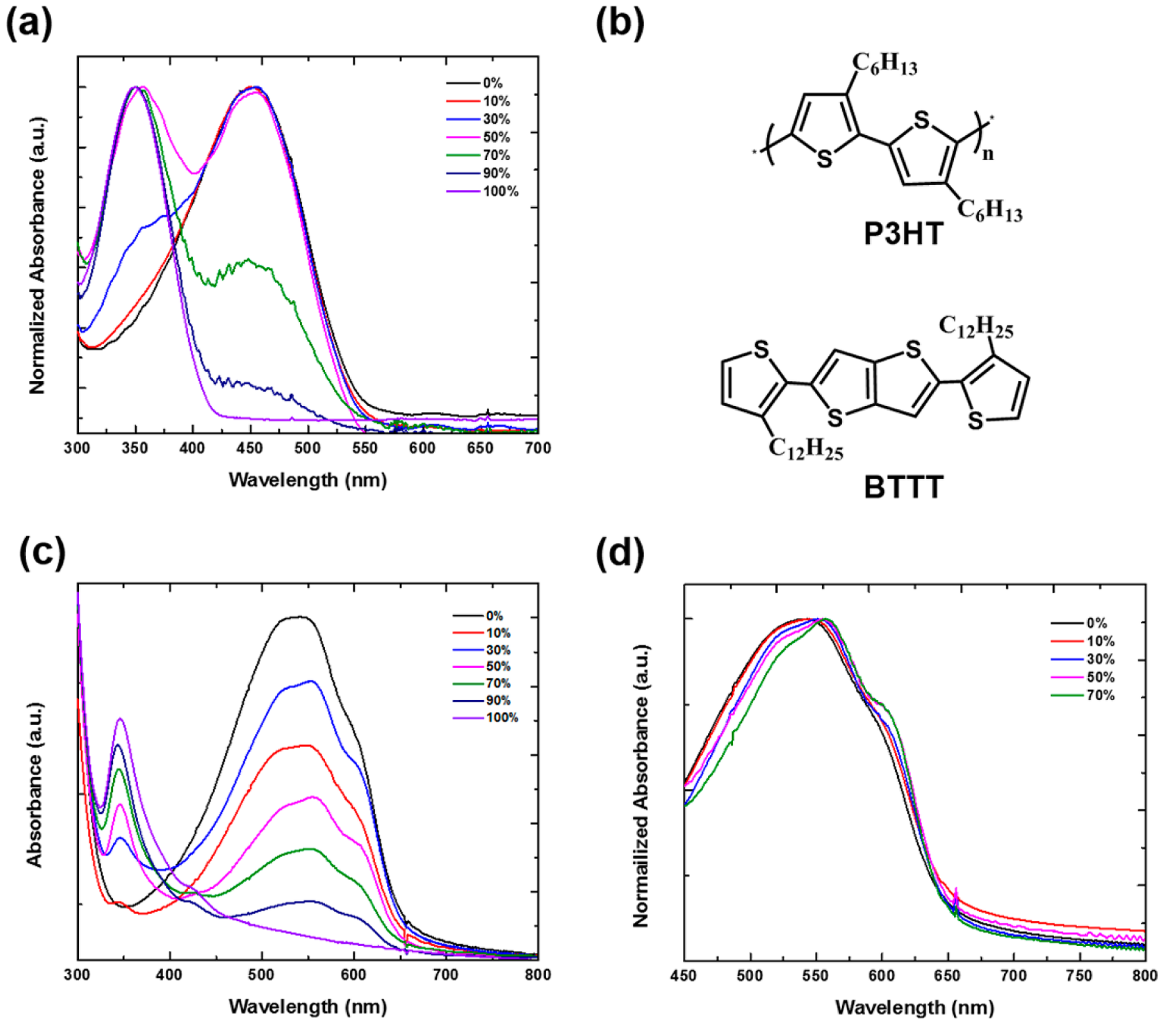

Figure 1. (a) Normalized UV−vis absorption spectra of P3HT:BTTT blend solutions with varying P3HT:BTTT blend ratio. (b) Molecular structures of P3HT and BTTT. (c) UV−vis absorption spectra and (d) normalized UV−vis absorption spectra of P3HT:BTTT blend thin films with different blend percentages of BTTT with respect to P3HT. (The normalized absorption bands for 90 and 100% blend thin films are not provided because the peaks at ca. 550 nm are too small or absent.)

polydispersity, which lead to a decrease in crystallinity can negatively impact charge carrier mobility.[14,15] A straightforward approach to address these problems is to blend oligomer and polymer semiconducting materials to take advantage of the attributes of both components, while concomitantly compensating for the disadvantages. The resultant blend thin films are expected to combine the high crystallinity of the oligomers with the morphological features and interchain connectivity associated with the polymer component.

The polymer−oligomer blend approach was first reported by Russell et al.,[16] who showed that P3HT thin-film mobility can be enhanced almost 10-fold by incorporating the conjugated oligomer, dihexyl-quarterthiophene (DH4T). These devices exhibited a pronounced mobility enhancement as the DH4T concentration increased from 20 to 35 wt %. The mobility saturated (μ_{FET} = 0.01 cm^2/(V s)) when P3HT was blended with 50 wt % DH4T. The improved charge-transport performance was ascribed to the formation of oligomer crystals embedded in the polymer matrix, while effective charge-transport percolation pathways formed. In another study, Orgiu et al.[17] demonstrated that charge carrier mobility of P3HT increases when the semiconducting oligomer, 5,5′-bis(4-*n*-hexylphenyl)-2,2′-bithiophene (dH-PTTP), is codeposited with the polymer. Mansouri and co-workers[18] further investigated the photosensing and electrical properties of organic thin-film transistors based on the blend of TIPS-pentacene and P3HT prepared by solution processing. Recent work by Gemayel et al.[19] proposed a new strategy to improve transistor performance and showed the potential for P3HT:graphene nanoribbon (GNR) blends.

Although the results reported to date showed that field-effect mobilities can be improved through a polymer−oligomer blend approach, a number of serious issues remain: a high threshold voltage (V_{th}) ($|V_{th}| > 10$ V), or need for additional pre- or post-treatments to avoid the compromising V_{th} and on−off current ratio (I_{on}/I_{off}) are representative examples. Low V_{th} is required for devices to be compatible with the operating voltages of low power consumption logic circuits and portable electronic devices. However, control of V_{th} to a value close to zero remains difficult.

Herein, the conjugated oligothiophene, BTTT (Figure 1b), is incorporated into P3HT thin films with the aim of improving overall semiconducting performance, not only as measured by mobility, but also by V_{th} and I_{on}/I_{off} ratio. BTTT was selected as the oligomeric small molecule component due to its planar symmetrical fused aromatic rigid frame, i.e., thieno[3,2-

DOI: 10.1021/am509090j
ACS Appl. Mater. Interfaces 2015, 7, 6652−6660

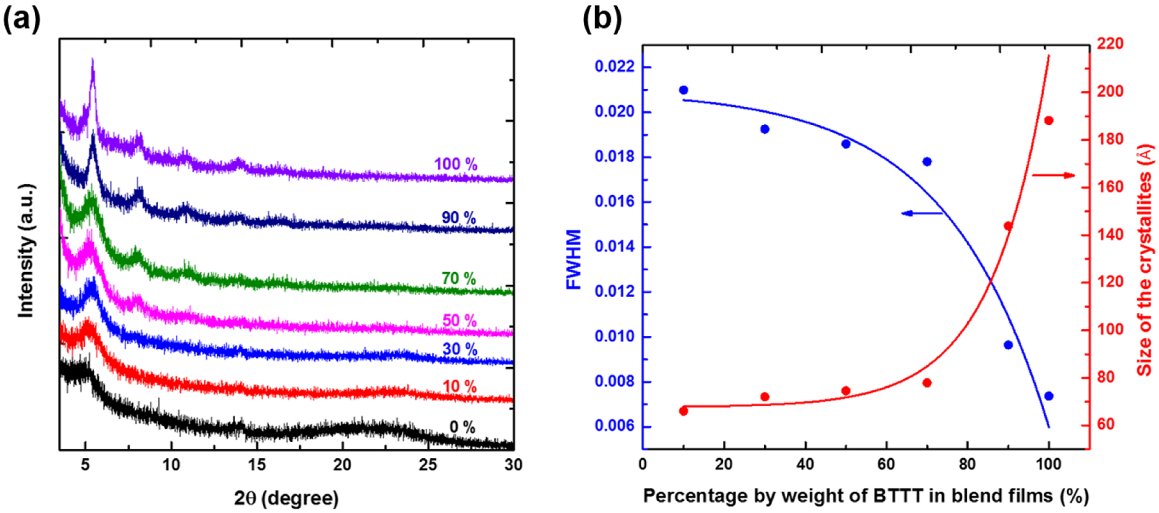

Figure 2. (a) GIXD profiles of P3HT:BTTT blend thin films with varying additional oligomer concentrations. (b) fwhm of (100) peaks and corresponding size of crystallites as a function of P3HT:BTTT blend ratio.

b]thiophene, which promotes the formation of highly ordered crystalline domains. Also, relative to the thiophene ring structure of P3HT, the thienothiophene is more stable with regards to oxidation. Blended thin films were deposited in the absence of electrode or dielectric treatment with self-assembled monolayers or post-treatments such as thermal annealing. All thin-film deposition processing was conducted under ambient conditions using a volatile, low boiling point solvent. These features are compatible with solution processing under nonstringent fabrication conditions and high-throughput processing.

RESULTS AND DISCUSSION

The optical absorption spectra obtained from P3HT:BTTT solution and corresponding blend thin films were measured by UV−vis spectroscopy as shown in Figure 1. In solution (Figure 1a), pristine P3HT (0% BTTT) exhibits a single absorption maximum, λ_{max}, associated with the $\pi-\pi^*$ intraband transition at ca. 450 nm, consistent with previous reports.[20−22] For the 100% BTTT oligomer solution, λ_{max} appears at ca. 350 nm and does not overlap with the pristine P3HT absorbance. Both distinct absorption bands can be observed in the polymer-oligomer blend solutions and the peak intensities vary with the blend ratios. The P3HT absorption bands associated with vibronic structure showing a 0−0 transition at ca. 605 nm and a 0−1 vibronic sideband at ca.550 nm are absent in the solutions.[22−24]

In contrast to the solution results, P3HT:BTTT blend thin films exhibit notably different UV−vis spectral features (Figure 1c). The absorption bands at ca. 550 nm and ca. 340 nm represent the P3HT and BTTT $\pi-\pi^*$ intraband transitions, respectively. The ratios of these bands are consistent with the polymer:oligomer proportions. In addition, the P3HT absorption peaks show an apparent red-shift (from ca. 450 to ca. 550 nm) with respect to the corresponding solution state spectra due to a higher degree of polymer chain planarization in the solid state.[25,26] To gain insight into the development of the P3HT absorption bands, we normalized the bands at ca. 550 nm, as shown in Figure 1d. Unlike the identical solution state P3HT spectral features with different blend ratios, the absorption bands in the solid state display a bathochromic shift as a function of additional oligomer concentration, meanwhile the weak absorption band at ca. 605 nm becomes progressively more pronounced. These features are both ascribed to enhancement of cofacial $\pi-\pi$ stacking and/or planarization of the conjugated backbone.[5,22,24]

The model by Spano enables a quantitative analysis of P3HT absorption spectra with respect to the analysis of intra- and intermolecular ordering of polymer chains.[26−28] The film absorption spectra are composed of a crystalline region because of ordered chains and an amorphous higher energy region due to disordered chains.[28] Within the crystalline regions, interchain coupling contributes to the formation of vibronic bands. The magnitude of interchain coupling can be estimated from the ratio of the 0−0 and 0−1 vibronic bands, which correlates with the free exciton bandwidth (W) of the aggregates.[24,28,29] A decrease of W can be ascribed to an increase in conjugation length and/or chain ordering. The values of W were calculated by the following eq 1.

$$\frac{I_{0-0}}{I_{0-1}} \approx \left(\frac{1 - 0.24W/E_p}{1 + 0.073W/E_p}\right)^2 \quad (1)$$

I_{0-0} and I_{0-1} represent the intensities of the 0−0 and 0−1 transitions, respectively obtained from fits to the experimental spectra (Figure S1a−e in the Supporting Information). E_p denotes the vibrational energy of the symmetric vinyl stretch at 0.18 eV.[26,28,29] The W value of both pristine P3HT and blend solutions could not be estimated since no aggregation was observed in the solution state. However, W for pristine P3HT thin film appears at 158.4 meV as shown in Figure S1f in the Supporting Information. Notably, this value continuously decreased to 93.35 meV with increased BTTT blend ratio up to 70%, suggesting that inclusion of the crystalline oligomer into the P3HT matrix may promote intermolecular ordering with increasing oligomer concentration.

Grazing incidence X-ray diffraction (GIXD) measurements were performed to confirm P3HT:BTTT blend thin-film microstructure as shown in Figure 2a. For pristine P3HT, the diffractogram presents a relatively weak and broad (100) peak associated with a lamellar packing structure of polymer chains,[30−32] and is indicative of either less ordering or an amorphous morphology. In contrast to the polymer thin film where crystallinity might be inhibited by chain entanglement,

DOI: 10.1021/am509090j
ACS Appl. Mater. Interfaces 2015, 7, 6652−6660

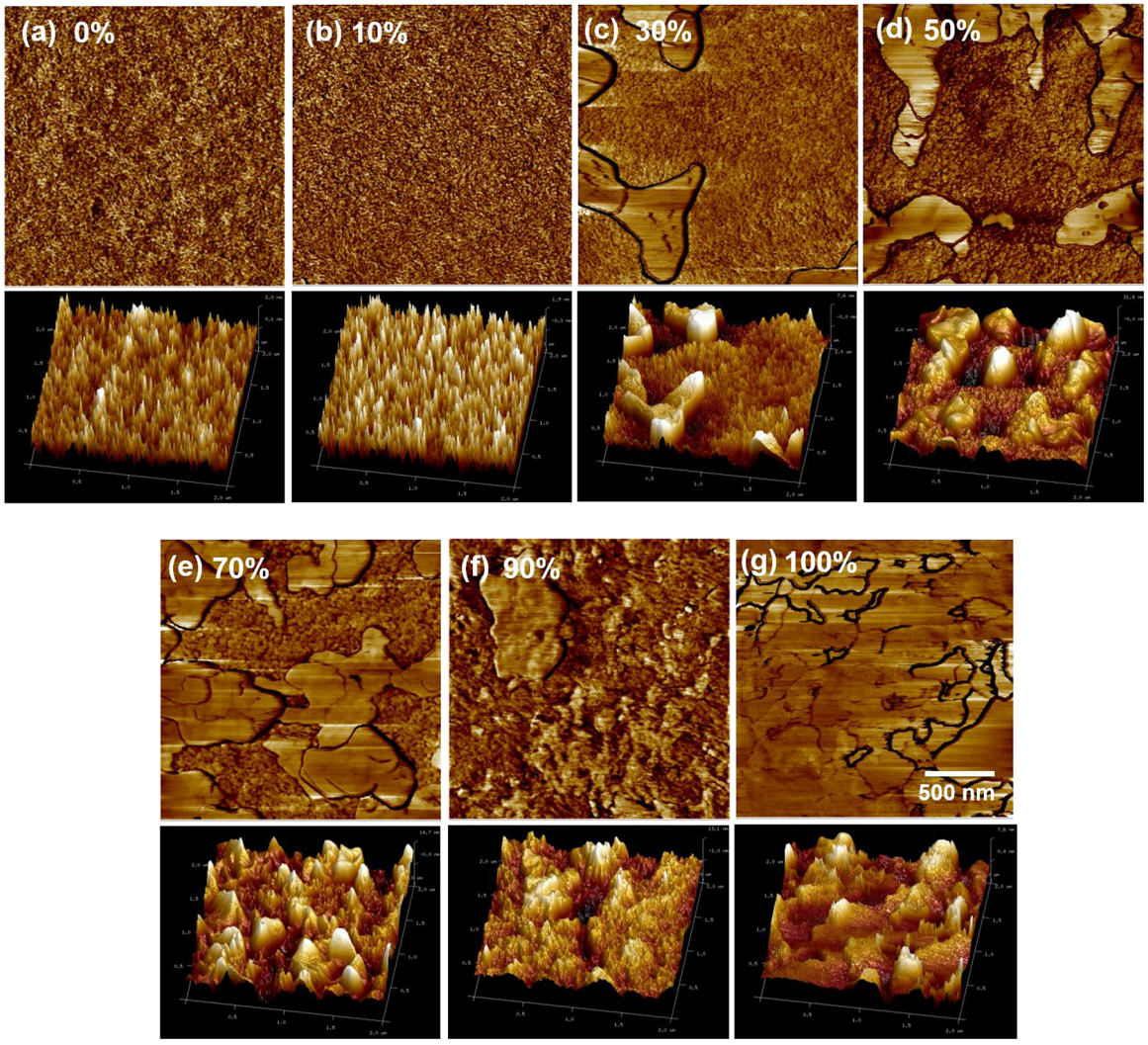

Figure 3. Tapping mode AFM phase images (upper) and corresponding 3D height images (lower) of P3HT:BTTT blend thin films, fabricating with a range of BTTT weight percentage in blend films (a) 0%, pristine P3HT, (b) 10%, (c) 30%, (d) 50%, (e) 70%, (f) 90%, (g) 100%, pristine BTTT. The scan area of all images was 2 × 2 μm.

chain folding, or polydispersity, oligomer or low-molecular-weight polymers crystallize more readily during rapid thin-film forming conditions such as spin coating.[14] Thus, it can be expected that addition of the oligomer led to an increase in (100) peak intensity, which could be ascribed to either an increase in individual crystal size, number of crystallites, or both.[23] Pure, drop-cast BTTT and P3HT thin films were also measured by GIXD as shown in Figure S6 in the Supporting Information. The results reveal that the pristine semiconductors exhibit diffraction peaks at 2θ = 5.40° (d-spacing = 16.35 Å) and 2θ = 5.43° (d-spacing =16.26 Å), respectively, which are in close proximity to each other. Overlap between the XRD peaks makes it difficult to evaluate the improvement of P3HT crystallinity in blend thin films. Fortunately, the P3HT and BTTT thin films show a distinct absorption band, which can provide an alternative perspective to evaluate polymer chain structural ordering in the two-component system. As discussed above, UV−vis spectral analysis suggests that not only does the crystalline BTTT contribute to the enhanced diffraction peaks of blends but the enhancement can also partially be attributed to improved P3HT ordering. The size of the crystalline domains could be further estimated using the Scherrer equation,[33,34] where λ is the incident X-ray wavelength, K is a crystallite-shape factor, θ is the Bragg angle, B is the full-width at half-maximum (fwhm) obtained from the X-ray diffraction peak in radians, and L represents the size of crystallites.

$$L = \frac{K\lambda}{B\cos\theta} \tag{2}$$

In the case of pristine P3HT thin films, the value of L could not be calculated because of the amorphous morphology. With an increase in BTTT weight percent, the (100) peak fwhm decreased. Thus, the calculated crystallite size grew from about 70 to roughly 180 Å as shown in Figure 2b.

P3HT:BTTT blend thin-film surface morphologies were investigated by tapping mode Atomic Force Microscopy (AFM). Phase and height images (2 × 2 μm) of the blends are presented in Figure 3 and Figure S2 in the Supporting Information, respectively. For pristine P3HT or blend thin films with low levels of BTTT, the topographic images appear featureless and lack texture, consistent with the amorphous structure observed through XRD analysis. However, islandlike features begins to appear and increase in size as the BTTT weight ratio rose over 30%. Concomitantly, surface roughness

DOI: 10.1021/am509090j
ACS Appl. Mater. Interfaces 2015, 7, 6652−6660

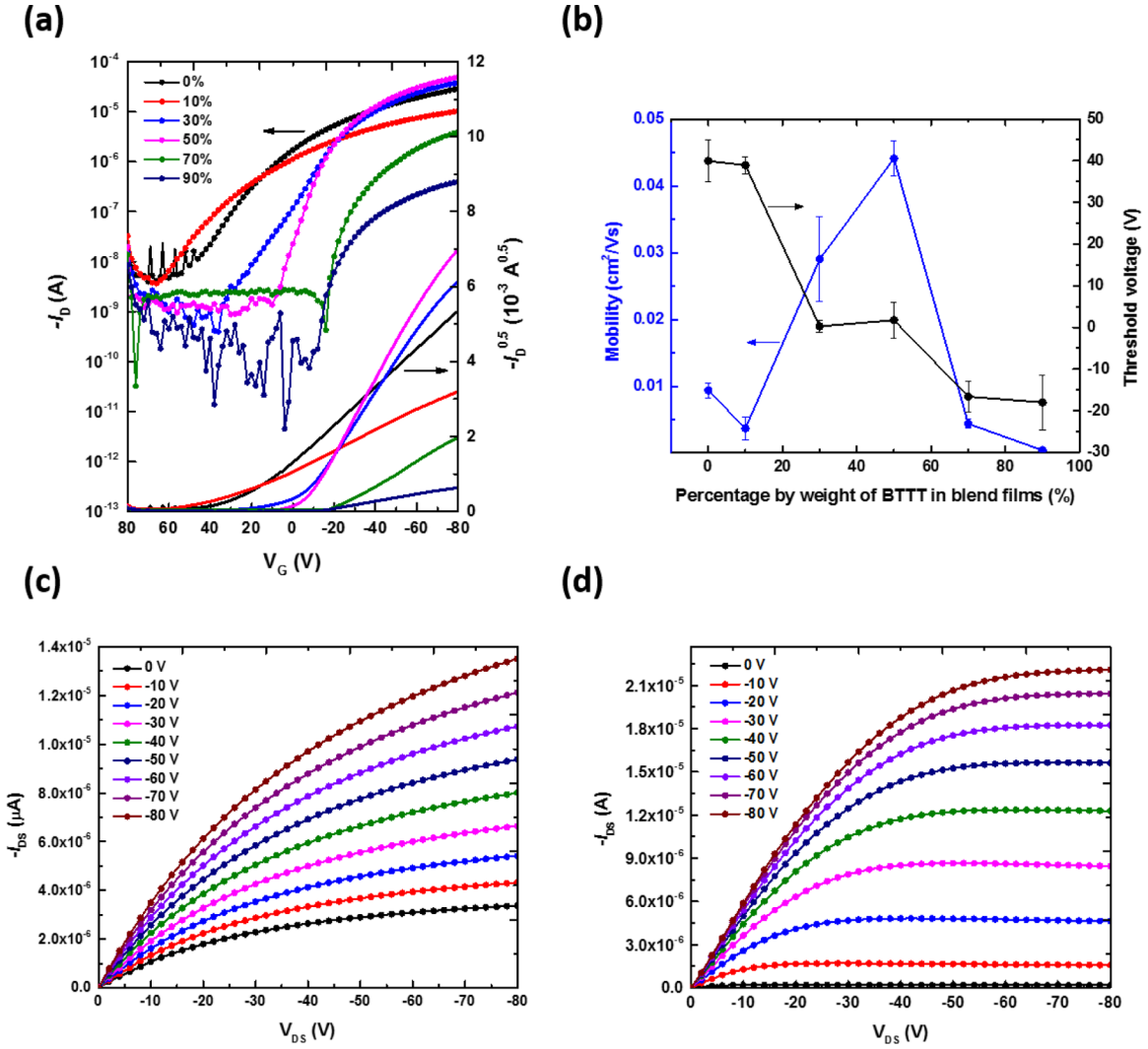

Figure 4. (a) Transfer characteristics of P3HT:BTTT blend OFET devices with different blend percentages of BTTT with respect to P3HT (V_D = −80 V). (b) Average field-effect mobility and threshold voltage obtained from P3HT:BTTT blend OFET devices as a function of oligomer concentrations. Output characteristics of (c) pristine P3HT and (d) 50% P3HT:BTTT blend thin film measured from different gate voltage (V_G = 0 to −80 V).

increased from 0.6 to 9.7 nm as shown in Figure S3 in the Supporting Information, in further support of increased thin-film crystallinity and molecular ordering. The images suggest that the polymer:oligomer blend thin films are comprised of crystals separated by an amorphous matrix. Increasing the oligomer fraction further, the crystal size became larger and then near 100%, evolved into a terracelike film structure with decreased surface roughness (9.7 to 3.9 nm). It is worth noting that although pristine BTTT shows a highly ordered structure compared to pristine P3HT or blended thin films, the crystal size is not sufficient to fully cover the active channel (50 μm). Thus, charge transport between source and drain electrodes may be limited because of the large number of grain boundaries, and lack of interconnectivity between domains.

The charge-carrier transport properties of P3HT:BTTT blend thin films were investigated by spin coating respective blend solutions onto bottom-gate bottom-contact field-effect transistor substrates. The channel length and width between source and drain gold electrodes was 50 μm and 2 mm, respectively. Figure 4a, c, d depicts the transfer and output curves for devices fabricated with P3HT:BTTT blends, and the resulting average mobilities, as a function of the BTTT weight percent, are presented in Figure 4b. The average mobility was calculated in the saturation regime at −80 V drain voltage.

As shown in Figure 4b, the pristine P3HT thin film exhibited a mobility ($9.37 \pm 1.00 \times 10^{-3}$ $cm^2/(V\,s)$) and large threshold voltage (40.0 ± 5.0 V). All devices were fabricated under ambient conditions with no electrode/dielectric surface treatment or postdeposition processing such as thermal annealing were employed. Hence, residual doping and/or acceptor-like traps at the P3HT-oxide interface are inevitable and are likely responsible for the high threshold voltage.[35,36] In other words, a decrease in carrier trap density is favorable for decreasing the threshold voltage. However, P3HT is very susceptible to atmospheric oxygen due to its relatively low ionization potential (IP).[37−39] Thus, some oxygen is expected to diffuse into the P3HT thin films generating a P3HT-O_2 complex, which can act as a charge carrier trap and lead to a positive shift in threshold voltage.[40−44]

The semiconducting performance did not show any improvement upon addition of a small quantity of BTTT (10%). However, the charge carrier mobility was enhanced

DOI: 10.1021/am509090j
ACS Appl. Mater. Interfaces 2015, 7, 6652−6660

approximately 5-fold with a BTTT weight ratio up to 50%. Significantly, the threshold voltage decreased from 40.0 ± 5.0 V to 1.7 ± 4.3 V, whereas the current on/off ratio improved from 1×10^4 to 1×10^5 as shown in Figure 4a-b. Additionally, the output characteristics of the 1:1 P3HT:BTTT blend thin film presents apparently different features with respect to pristine P3HT, which showed only partial saturation. An ideal OFET should enter the saturation region when $V_D \geq (V_G - V_T)$. In other words, further increases in V_D should yield no additional drain current. As shown in Figure 4c, pristine P3HT devices exhibit much higher drain currents with no applied gate voltage (V_G = 0 V), suggesting a significant parasitic bulk conductivity.[42] Horowitz et al.[44] revealed that this "ohmic" current behavior in pristine P3HT devices can be ascribed to p-doping of the mobile impurities in polythiophene, particularly since all device fabrication was carried out under ambient conditions. These mobile dopants are likely to migrate in the electric field, resulting in nonsaturated drain current. In contrast, the issues associated with p-doping were markedly diminished when 50% BTTT was incorporated into the P3HT thin film and afforded saturated output characteristics as shown in Figure 4d.

The device characterization results are consistent with UV−vis and XRD data demonstrating increased molecular ordering upon incorporation of the crystalline oligomer BTTT into P3HT thin films leading to more effective charge carrier transport pathways. Also, because a larger fraction of oxygen sensitive P3HT was substituted with the air-stable crystalline oligomers having relatively deep highest occupied molecular orbitals (HOMO), the blend thin films acquired greater resistance against oxidative doping, resulting in a substantial decrease in threshold voltage and increase in on/off ratio.

In order to further confirm the above assumption, the intrinsic work function (ϕ) and IP of the parent semiconductors and their respective blends were determined by ultraviolet photoelectron spectroscopy (UPS). The UPS spectra and corresponding IP for the blend thin films are provided in Figure S4 in the Supporting Information and Figure 5, respectively. The pristine P3HT thin film exhibited a relatively low IP at 4.57 ± 0.07 eV, in agreement with previously reported results.[45,46] In contrast, the IP for BTTT is at about 5.20 ± 0.02 eV, approximately 0.6 eV higher than the conjugated polymer, suggesting greater environmental stability. For the blends, the UPS spectra for the onset of the secondary electron cut off energy, shift to a lower binding energy as the BTTT weight ratio increased (Figure S4 in the Supporting Information). This shift is indicative of a deeper HOMO energy level and concomitant reduction in the impact of unintentional oxidative doping, which could severely deteriorate device charge-transport performance.

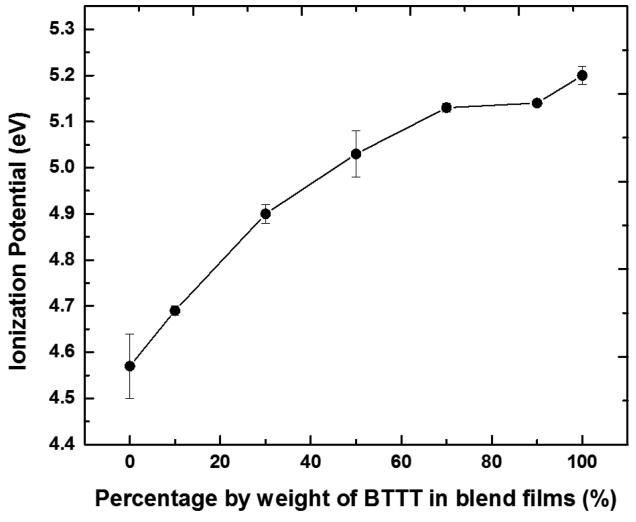

Figure 5. Ionization potential of P3HT:BTTT blend thin films as a function of the weight percentage of BTTT with respect to P3HT in the blend films.

Device performance peaks at a 1:1 blend ratio, followed by an abrupt decrease in thin-film mobility upon further increases in the fraction of BTTT. From XRD analysis, the highest crystallinity of the blend thin films was observed when the oligomer concentration exceeded 90%. Nevertheless, the 90% blend exhibited inferior charge-transport performance, and no macroscopic mobility could be measured from solution processed, pristine BTTT thin films. Zheng et al.[47] demonstrated that a pristine BTTT thin film exhibits charge-transport properties when the high boiling point solvent, chlorobenzene (bp = 131 °C) was used for device fabrication. However, the mobility was limited by rapid solvent evaporation during solution processing. The deterioration of OFET performance when the oligomer became the majority component of the blend thin film will be further discussed below.

Scheme 1 presents a schematic illustration of the evolution of thin-film morphology for P3HT:BTTT blends as the oligomer weight ratio increases. UV−vis, XRD, and AFM results suggest that the molecular ordering of a pristine P3HT thin film is inhibited by intrinsic polymer properties such as long-chain entanglement during the kinetically limited spin coating process which results in poor charge-transport performance. As an appropriate amount of BTTT is incorporated into the P3HT thin films, island-like crystal domains appear, and are embedded in an amorphous matrix. Meanwhile, the long polymer chains can serve as interconnection pathways between crystalline domains, which are isolated by disordered regions. The interconnecting polymer chains minimize the possibility that charge carriers will be trapped at grain boundaries. Above the optimum blend ratio, further increase in the proportion of BTTT leads to a negative impact on charge transport. The deterioration in semiconducting performance can be ascribed to two root causes. First, as observed from the AFM images (Figure 3), there are a relatively large number of grain boundaries present in thin films prepared with a high proportion of BTTT. Kelley et al.[48] demonstrated that the presence of grain boundaries produce an energy barrier and increase contact resistance, hence preventing effective charge transport between grains. Second, P3HT polymer chains, which can bridge and connect the large crystal domains are absent in the high oligomer concentration thin films, thereby severely limiting the formation of charge percolation paths between crystals. These results confirm that crystallinity is, in and of itself, insufficient for effective macroscopic organic/polymer charge carrier transport performance, and increased connectivity between the crystalline domains must also be considered.[13,49]

CONCLUSION

In conclusion, the overall macroscopic charge carrier transport performance of a representative solution processable, polymer semiconductor, P3HT, was significantly improved through a

DOI: 10.1021/am509090j
ACS Appl. Mater. Interfaces 2015, 7, 6652−6660

Scheme 1. Suggested Schematic Illustration of the Evolution of P3HT:BTTT Blend Thin-Films As a Function of the Proportion of BTTT

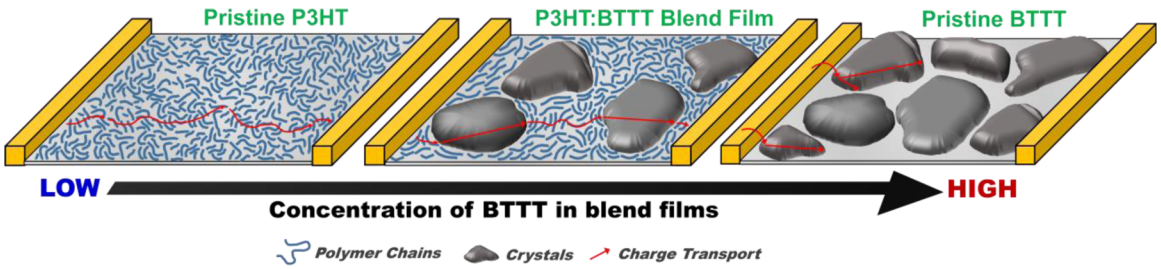

blend approach where the oligomer BTTT was incorporated into the polymer thin films. The surface morphology and thin-film crystallinity was tunable by varying the weight fraction of oligomer. The macroscopic charge carrier transport properties, as determined by OFET performance, were optimum at a 1:1 blend ratio because of synergistic effects in the two-component system. The incorporation of the crystalline oligomer into P3HT is favorable for the formation of supramolecular ordered morphologies during the rapid thin-film formation process. Meanwhile, the presence of the long chain polymer appears to reduce the negative impact of grain boundaries between small crystalline domains, leading to more effective charge hopping between transport sites. Furthermore, the remarkable decrease in V_{th} in the absence of surface treatment or annealing steps underscores the advantages of this approach for low-cost, large-area, flexible electronics fabrication.

EXPERIMENTAL SECTION

Materials. The P3HT (Mw: 60k, PDI: 1.9 RR: 96%) and chloroform (anhydrous grade) were purchased from Rieke Metals Inc. and Sigma-Aldrich, respectively, and used without further purification. The BTTT was synthesized according to the literature procedure.[47]

Organic Field-Effect Transistor (OFET) Fabrication and Characterization. The bottom-gate bottom-contact OFET substrates were fabricated using a heavily n- doped silicon wafer as the gate electrode. A 300 nm thick layer of thermally grown SiO_2 served as the gate dielectric. The 50 nm Au source and drain electrodes with 3 nm Cr as the adhesion layer were both deposited via standard photolithography based lift-off processing, followed by E-beam evaporation onto the SiO_2 layer. Before semiconducting layer deposition, all devices were cleaned in an ultrasound cleaning bath and sequentially rinsed with acetone, methanol and isopropanol. At the final step of the cleaning process, the devices were exposed to UV-ozone to ensure complete removal of residual photoresist and other organic contaminants. Before the thin-film formation process, pristine P3HT (0.33 wt %) and BTTT (0.33 wt %) solutions were prepared in $CHCl_3$ at ca. 55 °C with stirring. Subsequently, the respective blend solutions were prepared by mixing the defined ratios of the well-dissolved pristine P3HT and BTTT solutions as listed in Table S2 in the Supporting Information. The fabrication of OFET devices was completed by spin-coating P3HT:BTTT blend solutions onto the precleaned substrates under ambient condition.

All OFET electrical properties were tested using an Agilent 4155C semiconductor parameter analyzer. The field-effect mobilities, threshold voltage and current on−off ratios were calculated in the saturation regime (V_{DS} = −80 V) from the transfer plot of V_G versus I_{DS} and using the following equation

$$I_{DS} = \frac{WC_{ox}}{2L}\mu(V_{GS} - V_{th})^2 \quad (3)$$

where W and L refer to the channel length (50 μm) and width (2 mm), respectively, μ represents the hole mobility, V_{th} is the threshold voltage, and C_{ox} is the capacitance per unit area of the SiO_2 gate dielectric (1.15×10^{-8} F/cm^2).

UV−Vis Spectroscopy. The solution and solid state UV−vis spectra were measured by using an Agilent HP 8510 UV−vis spectrophotometer. The thin films for the solid-state studies were prepared by spin coating the relevant solution onto precleaned glass slides, which had undergone the same clean procedure as indicated above for OFET devices.

Grazing Incidence X-ray Diffraction (GIXD). Out-of-plane grazing incidence X-ray diffractograms were collected using a Panalytical X'Pert Pro system equipped with a Cu K_a X-ray irradiation source (λ = 1.541 Å), and operating at 45 kV and 40 mA. The X-ray incidence angle was fixed at 0.2° and the detector was scanned from 3 to 30°. The samples for GIXD characterization were prepared by spin-coating relevant solutions onto silicon substrates, having a 300 nm silicon oxide layer.

Atomic Force Microscopy (AFM). The surface morphology of the blend thin films with different blend ratios were characterized by AFM using a Bruker Dimension Icon atomic force microscopy system, operating in tapping mode with a silicon tip (TAP150, Bruker).

Ultraviolet Photoelectron Spectroscopy (UPS). Ultraviolet Photoelectron Spectra were obtained on a Kratos Axis Ultra DLD XPS/UPS system, using a 21.2 eV He-ion UV light source. The UPS data were recorded at a 5 eV pass energy and 0.05 eV step size with the spot diameter set to 55 μm. The ionization potential (IP = −HOMO) and work function (ϕ) were calculated by the following eqs 4 and 5

$$\mathrm{IP} = h\nu - (E_{cutoff} - \varepsilon_V^F) \quad (4)$$

$$Ø = h\nu - E_{cutoff} \quad (5)$$

where $h\nu$, E_{cutoff}, ε_V^F denote the incident photo energy (He I, 21.2 eV), the secondary electron cutoff energy value, and the lowest binding energy point, respectively.

ASSOCIATED CONTENT

Supporting Information

The results of fits to UV−vis spectra, AFM height images, surface roughness, UPS spectra, XRD patterns of drop cast thin film, table of ionization potential of P3HT:BTTT blend thin films, and transfer characteristics of pristine P3HT fabricated under nitrogen conditions are discussed. This material is available free of charge via the Internet at http://pubs.acs.org/.

AUTHOR INFORMATION

Corresponding Author

*E-mail: ereichmanis@chbe.gatech.edu.

Notes

The authors declare no competing financial interest.

ACKNOWLEDGMENTS

The financial support of Georgia Institute of Technology and the Air Force Office of Scientific Research (FA9550-12-1-0248) is gratefully acknowledged. L.Z., N.S.C., and A.L.B thank the

DOI: 10.1021/am509090j
ACS Appl. Mater. Interfaces 2015, 7, 6652−6660

National Science Foundation (DMR-1112455, CMMI-0531171) and the Office of Naval Research (N0001471410053).

REFERENCES

(1) Søndergaard, R.; Hösel, M.; Angmo, D.; Larsen-Olsen, T. T.; Krebs, F. C. Roll-to-Roll Fabrication of Polymer Solar Cells. *Mater. Today* **2012**, *15*, 36−49.

(2) Cantatore, E.; Geuns, T. C. T.; Gelinck, G. H.; van Veenendaal, E.; Gruijthuijsen, A. F. A.; Schrijnemakers, L.; Drews, S.; de Leeuw, D. M. A 13.56-MHz RFID System Based on Organic Transponders. *IEEE J. Solid-State Circuits* **2007**, *42*, 84−92.

(3) Ji, D.; Jiang, L.; Cai, X.; Dong, H.; Meng, Q.; Tian, G.; Wu, D.; Li, J.; Hu, W. Large Scale, Flexible Organic Transistor Arrays and Circuits Based on Polyimide Materials. *Org. Electron.* **2013**, *14*, 2528−2533.

(4) Hammock, M. L.; Knopfmacher, O.; Ng, T. N.; Tok, J. B. H.; Bao, Z. Electronic Readout Enzyme-Linked Immunosorbent Assay with Organic Field-Effect Transistors as a Preeclampsia Prognostic. *Adv. Mater.* **2014**, *26*, 6138−6144.

(5) Chang, M.; Choi, D.; Fu, B.; Reichmanis, E. Solvent Based Hydrogen Bonding: Impact on Poly(3-hexylthiophene) Nanoscale Morphology and Charge Transport Characteristics. *ACS Nano* **2013**, *7*, 5402−5413.

(6) Wie, J. J.; Nguyen, N. A.; Cwalina, C. D.; Liu, J.; Martin, D. C.; Mackay, M. E. Shear-Induced Solution Crystallization of Poly(3-hexylthiophene) (P3HT). *Macromolecules* **2014**, *47*, 3343−3349.

(7) Aiyar, A. R.; Hong, J. I.; Izumi, J.; Choi, D.; Kleinhenz, N.; Reichmanis, E. Ultrasound-Induced Ordering in Poly(3-hexylthiophene): Role of Molecular and Process Parameters on Morphology and Charge Transport. *ACS Appl. Mater. Interfaces* **2013**, *5*, 2368−2377.

(8) Zen, A.; Pflaum, J.; Hirschmann, S.; Zhuang, W.; Jaiser, F.; Asawapirom, U.; Rabe, J. P.; Scherf, U.; Neher, D. Effect of Molecular Weight and Annealing of Poly(3-hexylthiophene)s on the Performance of Organic Field-Effect Transistors. *Adv. Funct. Mater.* **2004**, *14*, 757−764.

(9) Kline, R. J.; McGehee, M. D.; Kadnikova, E. N.; Liu, J.; Fréchet, J. M. J.; Toney, M. F. Dependence of Regioregular Poly(3-hexylthiophene) Film Morphology and Field-Effect Mobility on Molecular Weight. *Macromolecules* **2005**, *38*, 3312−3319.

(10) Zhang, R.; Li, B.; Iovu, M. C.; Jeffries-El, M.; Sauvé, G.; Cooper, J.; Jia, S.; Tristram-Nagle, S.; Smilgies, D. M.; Lambeth, D. N.; McCullough, R. D.; Kowalewski, T. Nanostructure Dependence of Field-Effect Mobility in Regioregular Poly(3-hexylthiophene) Thin Film Field Effect Transistors. *J. Am. Chem. Soc.* **2006**, *128*, 3480−3481.

(11) Himmelberger, S.; Vandewal, K.; Fei, Z.; Heeney, M.; Salleo, A. Role of Molecular Weight Distribution on Charge Transport in Semiconducting Polymers. *Macromolecules* **2014**, *47*, 7151−7157.

(12) Sirringhaus, H.; Brown, P. J.; Friend, R. H.; Nielsen, M. M.; Bechgaard, K.; Langeveld-Voss, B. M. W.; Spiering, A. J. H.; Janssen, R. A. J.; Meijer, E. W.; Herwig, P.; de Leeuw, D. M. Two-Dimensional Charge Transport in Self-Organized, High-Mobility Conjugated Polymers. *Nature* **1999**, *401*, 685−688.

(13) Kline, R. J.; McGehee, M. D.; Kadnikova, E. N.; Liu, J.; Fréchet, J. M. J. Controlling the Field-Effect Mobility of Regioregular Polythiophene by Changing the Molecular Weight. *Adv. Mater.* **2003**, *15*, 1519−1522.

(14) Zhang, L.; Colella, N. S.; Liu, F.; Trahan, S.; Baral, J. K.; Winter, H. H.; Mannsfeld, S. C. B.; Briseno, A. L. Synthesis, Electronic Structure, Molecular Packing/Morphology Evolution, and Carrier Mobilities of Pure Oligo-/Poly(alkylthiophenes). *J. Am. Chem. Soc.* **2013**, *135*, 844−854.

(15) Smith, J.; Hamilton, R.; McCulloch, I.; Stingelin-Stutzmann, N.; Heeney, M.; Bradley, D. D. C.; Anthopoulos, T. D. Solution-Processed Organic Transistors Based on Semiconducting Blends. *J. Mater. Chem.* **2010**, *20*, 2562−2574.

(16) Russell, D. M.; Newsome, C. J.; Li, S. P.; Kugler, T.; Ishida, M.; Shimoda, T. Blends of Semiconductor Polymer and Small Molecular Crystals for Improved-Performance Thin-Film Transistors. *Appl. Phys. Lett.* **2005**, *87*, 222109.

(17) Orgiu, E.; Masillamani, A. M.; Vogel, J.-O.; Treossi, E.; Kiersnowski, A.; Kastler, M.; Pisula, W.; Dotz, F.; Palermo, V.; Samori, P. Enhanced Mobility in P3HT-Based OTFTs upon Blending with a Phenylene-thiophene-thiophene-phenylene Small Molecule. *Chem. Commun.* **2012**, *48*, 1562−1564.

(18) Mansouri, S.; Mir, L. E.; Al-Ghamdi, A. A.; Al-Hartomy, O. A.; Said, S. A. F. A.; Yakuphanoglu, F. Characterization and Modeling of TIPS-pentacene-poly(3-hexyl) Thiophene Blend Organic Thin Film Transistor. *Synth. Met.* **2013**, *185*−*186*, 153−158.

(19) El Gemayel, M.; Narita, A.; Dossel, L. F.; Sundaram, R. S.; Kiersnowski, A.; Pisula, W.; Hansen, M. R.; Ferrari, A. C.; Orgiu, E.; Feng, X.; Mullen, K.; Samori, P. Graphene Nanoribbon Blends with P3HT for Organic Electronics. *Nanoscale* **2014**, *6*, 6301−6314.

(20) Wu, P.-T.; Xin, H.; Kim, F. S.; Ren, G.; Jenekhe, S. A. Regioregular Poly(3-pentylthiophene): Synthesis, Self-Assembly of Nanowires, High-Mobility Field-Effect Transistors, and Efficient Photovoltaic Cells. *Macromolecules* **2009**, *42*, 8817−8826.

(21) Berson, S.; De Bettignies, R.; Bailly, S.; Guillerez, S. Poly(3-hexylthiophene) Fibers for Photovoltaic Applications. *Adv. Funct. Mater.* **2007**, *17*, 1377−1384.

(22) Rughooputh, S. D. D. V.; Hotta, S.; Heeger, A. J.; Wudl, F. Chromism of Soluble Polythienylenes. *J. Polym. Sci., Part B: Polym. Phys.* **1987**, *25*, 1071−1078.

(23) Aiyar, A. R.; Hong, J. I.; Nambiar, R.; Collard, D. M.; Reichmanis, E. Tunable Crystallinity in Regioregular Poly(3-Hexylthiophene) Thin Films and Its Impact on Field Effect Mobility. *Adv. Funct. Mater.* **2011**, *21*, 2652−2659.

(24) Abdelsamie, M.; Zhao, K.; Niazi, M. R.; Chou, K. W.; Amassian, A. In situ UV-Visible Absorption DuringSpin-Coating of Organic Semiconductors: A New Probe for Organic Electronics and Photovoltaics. *J. Mater. Chem. C* **2014**, *2*, 3373−3381.

(25) Brown, P.; Thomas, D.; Köhler, A.; Wilson, J.; Kim, J.-S.; Ramsdale, C.; Sirringhaus, H.; Friend, R. Effect of Interchain Interactions on the Absorption and Emission of Poly(3-hexylthiophene). *Phys. Rev. B: Condens. Matter Mater. Phys.* **2003**, *67*, 064203.

(26) Clark, J.; Silva, C.; Friend, R. H.; Spano, F. C. Role of Intermolecular Coupling in the Photophysics of Disordered Organic Semiconductors: Aggregate Emission in Regioregular Polythiophene. *Phys. Rev. Lett.* **2007**, *98*, 206406.

(27) Spano, F. C. Modeling Disorder in Polymer Aggregates: The Optical Spectroscopy of Regioregular Poly(3-hexylthiophene) Thin Films. *J. Chem. Phys.* **2005**, *12*, 234701.

(28) Clark, J.; Chang, J.-F.; Spano, F. C.; Friend, R. H.; Silva, C. Determining Exciton Bandwidth and Film Microstructure in Polythiophene Films Using Linear Absorption Spectroscopy. *Appl. Phys. Lett.* **2009**, *94*, 163306.

(29) Chang, M.; Lee, J.; Chu, P.-H.; Choi, D.; Park, B.; Reichmanis, E. Anisotropic Assembly of Conjugated Polymer Nanocrystallites for Enhanced Charge Transport. *ACS Appl. Mater. Interfaces* **2014**, *6*, 21541−21549.

(30) Aryal, M.; Trivedi, K.; Hu, W. Nano-Confinement Induced Chain Alignment in Ordered P3HT Nanostructures Defined by Nanoimprint Lithography. *ACS Nano* **2009**, *3*, 3085−3090.

(31) Chang, J.-F.; Sun, B.; Breiby, D. W.; Nielsen, M. M.; Sölling, T. I.; Giles, M.; McCulloch, I.; Sirringhaus, H. Enhanced Mobility of Poly(3-hexylthiophene) Transistors by Spin-Coating from High-Boiling-Point Solvents. *Chem. Mater.* **2004**, *16*, 4772−4776.

(32) Prosa, T. J.; Winokur, M. J.; Moulton, J.; Smith, P.; Heeger, A. J. X-ray Structural Studies of Poly(3-alkylthiophenes): An Example of An Inverse Comb. *Macromolecules* **1992**, *25*, 4364−4372.

(33) Jeong, S.; Kwon, Y.; Choi, B.-D.; Ade, H.; Han, Y. S. Improved Efficiency of Bulk Heterojunction Poly(3-hexylthiophene):[6,6]-phenyl-C61-butyric Acid Methyl Ester Photovoltaic Devices Using Discotic Liquid Crystal Additives. *Appl. Phys. Lett.* **2010**, *96*, 183305.

DOI: 10.1021/am509090j
ACS Appl. Mater. Interfaces 2015, 7, 6652−6660

(34) Holzwarth, U.; Gibson, N. The Scherrer Equation Versus the 'Debye-Scherrer Equation'. *Nat. Nanotechnol.* **2011**, *6*, 534−534.
(35) Ma, L.; Lee, W. H.; Park, Y. D.; Kim, J. S.; Lee, H. S.; Cho, K. High Performance Polythiophene Thin-Film Transistors Doped with Bery Small Amounts of An Electron Acceptor. *Appl. Phys. Lett.* **2008**, *92*, 063310.
(36) Horowitz, G.; Delannoy, P. An Analytical Model for Organic-Based Thin-Film Transistors. *J. Appl. Phys.* **1991**, *70*, 469−475.
(37) Hoshino, S.; Yoshida, M.; Uemura, S.; Kodzasa, T.; Takada, N.; Kamata, T.; Yase, K. Influence of Moisture on Device Characteristics of Polythiophene-Based Field-Effect Transistors. *J. Appl. Phys.* **2004**, *95*, 5088−5093.
(38) Ong, B. S.; Wu, Y. L.; Liu, P.; Gardner, S. High-Performance Semiconducting Polythiophenes For Organic Thin-Film Transistors. *J. Am. Chem. Soc.* **2004**, *126*, 3378−3379.
(39) Manceau, M.; Rivaton, A.; Gardette, J.-L.; Guillerez, S.; Lemaître, N. The Mechanism of Photo- and Thermooxidation of Poly(3-hexylthiophene) (P3HT) Reconsidered. *Polym. Degrad. Stab.* **2009**, *94*, 898−907.
(40) Kehrer, L. A.; Winter, S.; Fischer, R.; Melzer, C.; von Seggern, H. Temporal and Thermal Properties of Optically Induced Instabilities in P3HT Field-Effect Transistors. *Synth. Met.* **2012**, *161*, 2558−2561.
(41) Wang, S.; Tang, J.-C.; Zhao, L.-H.; Png, R.-Q.; Wong, L.-Y.; Chia, P.-J.; Chan, H. S. O.; Ho, P. K.-H.; Chua, L.-L. Solvent Effects and Multiple Aggregate States in High-Mobility Organic Field-Effect Transistors Based on Poly(bithiophene-alt-thienothiophene). *Appl. Phys. Lett.* **2008**, *93*, 162103.
(42) Wang, A.; Kymissis, I.; Bulovic, V.; Akinwande, A. I. Engineering Density of Semiconductor-Dielectric Interface States to Modulate Threshold Voltage in OFETs. *IEEE Trans. Electron Devices* **2006**, *53*, 9−13.
(43) Wang, G.; Swensen, J.; Moses, D.; Heeger, A. J. Increased Mobility from Regioregular Poly(3-hexylthiophene) Field-Effect Transistors. *J. Appl. Phys.* **2003**, *93*, 6137−6141.
(44) Horowitz, G. Origin of the "Ohmic" Current in Organic Field-Effect Transistors. *Adv. Mater.* **1996**, *8*, 177−179.
(45) Osikowicz, W.; de Jong, M. P.; Salaneck, W. R. Formation of the Interfacial Dipole at Organic-Organic Interfaces: C60/Polymer Interfaces. *Adv. Mater.* **2007**, *19*, 4213−4217.
(46) Xu, Z.; Chen, L.-M.; Chen, M.-H.; Li, G.; Yang, Y. Energy Level Alignment of Poly(3-hexylthiophene): [6,6]-phenyl C61 Butyric Acid Methyl Ester Bulk Heterojunction. *Appl. Phys. Lett.* **2009**, *95*, 013301.
(47) Zhang, L.; Liu, F.; Diao, Y.; Marsh, H. S.; Colella, N. S.; Jayaraman, A.; Russell, T. P.; Mannsfeld, S. C. B.; Briseno, A. L. The Good Host: Formation of Discrete 1-D Fullerene "Channels" in Well-Ordered Poly(2,5-bis(3-alkylthiophen-2-yl)thieno[3,2-b]thiophene) Oligomers. *J. Am. Chem. Soc.* **2014**, *136*, 18120−1813.
(48) Kelley, T. W.; Frisbie, C. D. Gate Voltage Dependent Resistance of a Single Organic Semiconductor Grain Boundary. *J. Phys. Chem. B* **2001**, *105*, 4538−4540.
(49) O'Connor, B. T.; Reid, O. G.; Zhang, X.; Kline, R. J.; Richter, L. J.; Gundlach, D. J.; DeLongchamp, D. M.; Toney, M. F.; Kopidakis, N.; Rumbles, G. Morphological Origin of Charge Transport Anisotropy in Aligned Polythiophene Thin Films. *Adv. Funct. Mater.* **2014**, *24*, 3422−3431.

DOI: 10.1021/am509090j
ACS Appl. Mater. Interfaces 2015, 7, 6652−6660